AAS 19-409

A DENSITY-BASED APPROACH TO THE PROPAGATION OF RE-ENTRY UNCERTAINTIES

Mirko Trisolini†, Camilla Colombo‡

The proposed study aims at implementing a density-based approach for the propagation of uncertainties in the initial conditions and parameters for the analysis and prediction of spacecraft re-entries. Using the continuity equation together with the re-entry dynamics, the joint probability distribution function of the uncertainties is propagated and the final uncertainties in the re-entry corridor, impact location, and casualty area are quantified. The paper considers uncertainties in the initial conditions at re-entry and in the ballistic coefficient of the satellite for different types of re-entry scenarios, studying the effects that such uncertainties have on the impact location and entry corridor.

INTRODUCTION

The present study proposes a methodology based on the use of the continuity equation for the analysis of re-entry scenarios under the presence of uncertainty in the initial conditions and parameters.

The study and prediction of re-entry trajectories is an extremely complex task. The accuracy of these predictions is influenced by many factors, such as the initial conditions (in the form of re-entry velocity, altitude, flight path angle, etc.), the ballistic coefficient of the object, the modelling of the atmosphere, the aerothermal heating experienced by the object, etc. Uncertainties are associated to these parameters; whether the uncertainties are related to the measurements or to the modelling methodology, they produce an effect on the evolution of the re-entry trajectory, which, in turns, translates into an uncertainty in the prediction of the re-entry corridor, impact location, and casualty area. Quantifying such uncertainties is important and can be very useful in multiple circumstances. Re-entering spacecraft and rocket bodies can pose risk to people and properties on the ground. Consequently, it is important to quantify uncertainties related to re-entry scenarios as to properly assess the probability of impact on areas of interest. In addition, the design of exploration probes on other planets such as Mars can strongly benefit from uncertainty analyses in order to improve the robustness of the design of the mission by enabling the assessment of landing footprint and impact location uncertainty[1].

The traditional procedure to assess uncertainties is a Monte Carlo-based dispersion analysis, where through a large number of simulations over randomly sampled initial conditions and parameters, the joint Probability Density Function (PDF) is estimated through a frequentist approach. Monte Carlo (MC) simulations are not particularly suited for uncertainty analysis as they can only estimate the values of the uncertainties. In addition, the results they provide are only as good as the number of simulations performed. In general, in fact, MC dispersion analyses require many simulations. Consequently, for high-dimensional and non-linear dynamics, such as the ones associated with re-entry scenarios, they become tremendously expensive.

On the other hand, the continuity equation allows the propagation of the probability density along with the dynamics of the system thus obtaining a step-by-step evolution of the actual density distribution[1]. Such a methodology directly compares to Monte Carlo simulations where, instead, the distribution is only approximated through a large number of realizations. While with MC methods we propagate individual realisation of the initial PDF, with a density-based approach we propagate the ensemble of realisations conserving the total probability mass in the phase space throughout the simulation. As the propagation involves

† PostDoctoral Researcher, Dipartimento di Scienze e Tecnologie Aerospaziali, Politecnico di Milano, Via La Masa 34, 20156 Milano MI, AIAA Member.
‡ PhD, Associate Professor, Dipartimento di Scienze e Tecnologie Aerospaziali, Politecnico di Milano, Via La Masa 34, 20156 Milano MI, AIAA Member.

the actual values of the density in the phase space, the density-based method, allow for a lower number of simulations with respect to a MC method.

The paper studies the effects of uncertainties in the initial conditions and in the ballistic coefficient of satellites for different types of re-entry scenarios, considering both shallow and steep re-entry conditions. The uncertainty in the ballistic coefficient is included as it can strongly influence the shape and evolution of the re-entry trajectory and of the landing location. In addition, the exact quantification of the ballistic coefficient at re-entry can be difficult to compute with high accuracy as it depends on the mass, cross-section and drag coefficient of the spacecraft. The mass of the spacecraft at disposal may be not completely known, as the exact amount of residual propellant can be difficult to assess. The cross-sectional area of the satellite may be also uncertain, as it is difficult to predict the exact motion of an uncontrolled satellite when it enters in contact with the upper layers of the atmosphere. In addition, even the exact value of the drag coefficient can be of difficult computation. Once the propagation of the uncertainties is performed, the results are used to compute the impact probability on ground and the dispersion of both the impact location and the footprint.

METHODOLOGY

Uncertainty propagation

The proposed methodology uses the continuity equation in order to propagate the initial joint probability distribution function related to the uncertainties in the initial conditions and parameters and assess its evolution throughout the re-entry process under the influence of the re-entry dynamics. The expression for the continuity equations is as follows[2,3]

$$\frac{\partial n(\mathbf{x},t)}{\partial t}+\nabla\cdot\mathbf{f}(\mathbf{x})=\dot{n}^{+}-\dot{n}^{-} \tag{1}$$

where $\nabla\cdot\mathbf{f}$ represents the forces acting on the system and takes into account slow, continuous phenomena such as gravity and atmospheric drag, and $\dot{n}^{+}-\dot{n}^{-}$ represents the fast and discontinuous events (i.e. sources and sinks). For the case in exam, the source and sink terms have been neglected. Knowing the initial probability density distribution *n*, Eq. (1) allow for the propagation of the density evolution in time. When applied to the propagation of probabilistic uncertainty in the initial conditions and parameters[1]. This is a Partial Differential Equation (PDE) with the joint probability distribution function (PDF) $n(\mathbf{x}, t)$ being the dependent variable. Such an equation regulates the conservation of the total probability mass of the joint PDF through its spatial-temporal evolution due to the forces acting on the system.

Eq. (1) can be solved using the Method Of the Characteristics[4] (MOC), where the partial differential equation is transformed into a set of Ordinary Differential Equations (ODE). As it is convenient to express the evolution of the re-entry trajectory using parameters such as the altitude, the relative velocity, and the flight path angle, we follow the approach to express the continuity equation in the phase space of the problem in exam, writing the divergence in rectangular coordinates[5]. Using this approach, the problem can be written in the phase space of the relevant parameters, directly implementing the expressions for their variation with time. In the generic case of *m* variables, Eq. (1) can be re-written in rectangular coordinates as follows

$$\frac{\delta n}{\delta t}+\frac{\delta n}{\delta\alpha_1}v_{\alpha_1}+\cdots+\frac{\delta n}{\delta\alpha_m}v_{\alpha_m}+\left[\frac{\delta v_{\alpha_1}}{\delta\alpha_1}+\cdots+\frac{\delta v_{\alpha_m}}{\delta\alpha_m}\right]n=0 \tag{2}$$

where the sink and source terms have been neglected. Applying the method of characteristics, the PDE can be reduced to the following system of ODEs

$$\begin{cases} \dfrac{dt}{ds} = 1 \\ \dfrac{d\alpha_1}{ds} = v_{\alpha_1}\left(\alpha_1,\ldots,\alpha_m\right) \\ \quad\vdots \\ \dfrac{d\alpha_m}{ds} = v_{\alpha_m}\left(\alpha_1,\ldots,\alpha_m\right) \\ \dfrac{dn}{ds} = -\left[\dfrac{\delta v_{\alpha_1}}{\delta\alpha_1} + \cdots + \dfrac{\delta v_{\alpha_m}}{\delta\alpha_m}\right]\cdot n\left(\alpha_1,\ldots,\alpha_m,t\right) \end{cases} \tag{3}$$

where s is the independent variable, in this case the time t. In this paper, the continuity equation is applied to the atmospheric re-entry of spacecraft, starting with the implementation of a three-state representation model[6]. The model describes the evolution of the re-entry trajectory through the temporal evolution of the altitude (h), velocity (v), and flight-path angle (γ) under the influence of the planet gravity and the atmospheric drag as follows

$$\begin{aligned} \dot{h} &= v\cdot\sin\left(\gamma\right) \\ \dot{v} &= -\frac{1}{2}\cdot\frac{\rho}{\beta}\cdot v^2 - g\cdot\sin\left(\gamma\right) \\ \dot{\gamma} &= \frac{v\cdot\cos\left(\gamma\right)}{R_p+h} - \frac{g}{v}\cdot\cos\left(\gamma\right) + \frac{1}{2}\cdot\frac{\rho}{\beta}\cdot\frac{C_L}{C_D}\cdot v \end{aligned} \tag{4}$$

where h is altitude, the ρ is the atmospheric density, g is the gravitational acceleration, β is the ballistic coefficient, R_p is the radius of the planet, C_L is the lift coefficient, and C_D is the drag coefficient. For the modelling of the atmosphere an exponential model has been adopted (Eq. (5)), while for the gravitational acceleration an inverse square model has been implemented (Eq. (6)).

$$\rho\left(h\right) = \rho_0\cdot\exp\left(\frac{H_2-h}{H_1}\right) \tag{5}$$

$$g\left(h\right) = \frac{G\cdot M_p}{\left(R_p+h\right)^2} \tag{6}$$

where ρ_0 is a reference atmospheric density, H_1 and H_2 are constants related to the atmosphere of the planet, M_p is the mass of the planet, and G is the universal gravitational constant.

Applying the method of characteristics to the re-entry problem specifying Eqs. (4) to (6) into Eq. (3), we obtain the following set of ordinary differential equations

$$\begin{cases} \dfrac{dh}{dt} = v\cdot\sin\left(\gamma\right) \\ \dfrac{dv}{dt} = -\dfrac{1}{2}\cdot\dfrac{\rho}{\beta}\cdot v^2 - g\cdot\sin\left(\gamma\right) \\ \dfrac{d\gamma}{dt} = \dfrac{v\cdot\cos\left(\gamma\right)}{R_p+h} - \dfrac{g}{v}\cdot\cos\left(\gamma\right) + \dfrac{1}{2}\cdot\dfrac{\rho}{\beta}\cdot\dfrac{C_L}{C_D}\cdot v \\ \dfrac{dn}{dt} = \left[\dfrac{\rho}{\beta}\cdot v + \sin\left(\gamma\right)\cdot\left(\dfrac{v}{R_p+h} - \dfrac{g}{v}\right)\right]\cdot n \end{cases} \tag{7}$$

In general, it is difficult to find an analytical solution for Eq. (7) (except for the trivial case of horizontal flight[1]), and the system has to be numerically integrated. The integration can be performed using a standard ODE solver such as the Runge-Kutta method with a specified time step. In such fashion, the time evolution of

the density in the considered phase space can be obtained for a specified set of time instants. As the solution for the re-entry problem is not analytical, it is necessary to sample the initial density distribution and to integrate the system of Eq. (7) for each one of the sampled points. An important aspect that must be underlined is that with the presented method the value of the uncertainty correspondent to each sample is the actual uncertainty value and not an estimation of it, as it would be the case for a Monte Carlo based method.

Density reconstruction

Subsequently, the distribution can be reconstructed at each time step by interpolating the scattered data over the phase space domain. It is important here to highlight that during the re-entry evolution, not only the density changes but also the phase-space volume changes and deforms. In particular, the rate of change of the phase-space volume is related to the divergence of the vector field **f** (last line of Eq. (7)), as it possible to observe from the last expression of Eq. (3). In the present work, the density reconstruction is performed using a linear interpolation that exploits the Delaunay triangulation[7] of the sampled points used in the integration of Eq. (7). The vertices of each simplex generated by the triangulation together with the probability density associated with it, is used to linearly interpolate for all the interpolation points lying inside the simplex[8].

RESULTS

To present the application of the described density-based approach to the re-entry of satellites, two test cases have been selected. The chosen test cases are a shallow and a steep Earth re-entry, whose initial conditions are summarized in Table 1. The shallow entry is referred to as Low Earth Orbit (LEO) re-entry as the conditions are typical for a natural, uncontrolled re-entry from a low Earth orbit, whereas the steep re-entry is referred to as Strategic re-entry as it represents a scenario where the aim is to more precisely pinpoint the impact location on Earth[6].

Table 1. Nominal initial conditions for the two re-entry scenarios considered.

Initial Conditions	LEO Re-entry	Strategic Re-entry
Altitude (km)	100	125
Velocity (km/s)	7.9	7.2
Flight Path Angle (deg)	-1.35	-30
Ballistic Coefficient (kg/m^2)	450	10000

For both scenarios, an Earth re-entry is performed; the values for the remaining parameters related to the re-entry simulation are summarised in Table 2.

Table 2. Values of the re-entry parameters for an Earth re-entry.

Parameter	Value
R_p	6378.1 km
ρ_0	1.215 kg/m^3
H_1	8.5 km
H_2	0 km

After specifying the nominal initial conditions for the re-entry simulations, the uncertainties related to the initial conditions and the parameter need to be specified. For the purpose of this work, a Gaussian uncertainty having a 10% variance has been considered for the three initial conditions (altitude, velocity, and flight path angle) and for the ballistic coefficient. In general, re-entries are difficult to predict, especially in the latest stages, as the phenomenon is dependent from many factors, such as the solar activity, the atmospheric density, the attitude of the spacecraft, etc. Consequently, considering the uncertainties characterising the initial conditions at re-entry is a very important aspect of re-entry predictions. In fact, such the initial conditions affect the landing site of the spacecraft and the thermal and mechanical loads it is exposed to. Alongside the initial conditions, a relevant parameter has been considered source of uncertainty that is the ballistic coefficient. In fact, it is usually difficult to effectively and precisely determine the ballistic coefficient of a satellite as it

depends on its attitude and on the atmospheric conditions (through the drag coefficient). At the end-of-life of a spacecraft, its attitude may be known if the satellite is still controlled and operational; however, in other cases, the satellite is not operational anymore and its attitude cannot be controlled or known a priori. Similarly, the drag coefficient usually comes from engineering relations and it is estimated reducing the spacecraft structure to that one of a simple geometrical object[9] (e.g. boxes and cylinders). Consequently, the uncertainty related to it can be significant and should be considered.

Figure 1 shows the results for the LEO re-entry simulations for 5000 initial samples. The images represent the evolution of the re-entry and of the uncertainties associated with it in the phase space of the problem (i.e. altitude, velocity, and flight path angle). The variation of the ballistic coefficient is represented by the size of the points in the scatter plot. Intuitively, the larger the point, the bigger is the ballistic coefficient. It is important here to mention that for this test case, the ballistic coefficient for each of the samples does not vary during the simulations. In other words, no mass loss is considered, at the moment, in the re-entry simulation. The four plots represent the evolution of the re-entry under uncertainties at different time instant: the top-left plot shows the uncertainties after 40 s, the top-right after 80 s, the bottom-left after 160 s, and the bottom-right after 240 s.

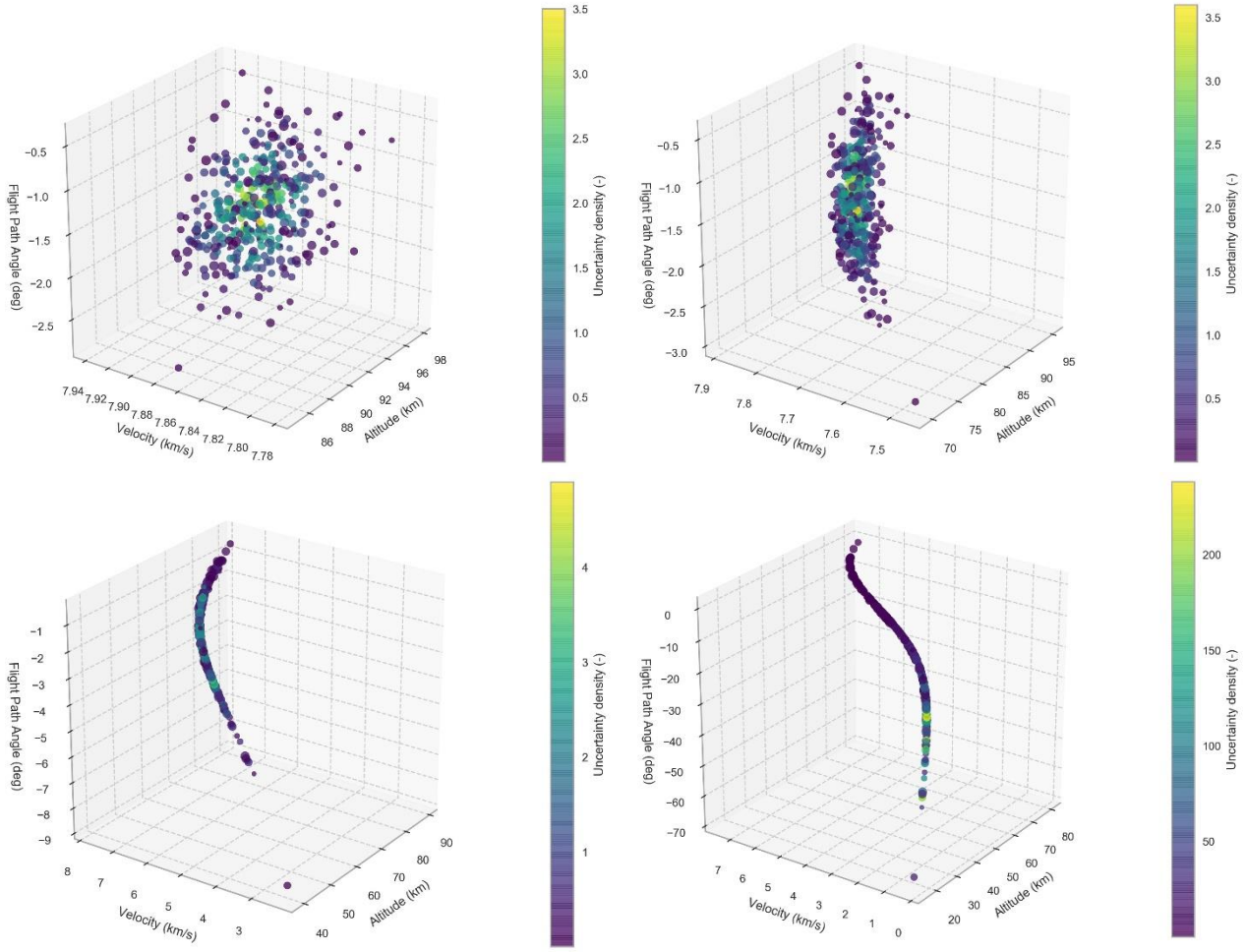

Figure 1. Scatter plot of the uncertainty evolution of the LEO re-entry case for the sampled initial conditions and parameters. The top-left plot represents the re-entry after 40 s, the top-right after 80 s, the bottom-left after 160 s, and the bottom-right after 240 s.

As it is possible to observe from Figure 1, the volume of the considered phase-space starts as relatively compact and maintains this property even after 80 s from the beginning of the re-entry phase. However, as the re-entry progresses, the volume of the phase-space stretches and elongates. We mention this characteristic of the phase-space as it is important in the reconstruction of the density at each time step and in the computation of the marginal probabilities associated to the re-entry parameters.

As an example, the one-dimensional marginal probability along the *x*-direction of a three-dimensional distribution function $\rho(x,y,z)$ is expressed by Eq. (8). Analogously, the two-dimensional marginal along *x* and *y* can be expressed by Eq. (9).

$$m_x = \iint \rho(x, y, z)\, dydz \tag{8}$$

$$m_{xy} = \int \rho(x, y, z)\, dz \tag{9}$$

The extension of the marginal computation to higher dimensions is trivial. All the marginal presented in this work have been computed using these expressions. However, as the probability density is only known at discrete points in the phase-space, the marginals are obtained by slicing the relevant axis into intervals; for each interval, only the interpolation points belonging to it are considered and the integrated to obtain the value of the marginal density at the specified interval.

The marginal probabilities are of interest for the re-entry simulations as they explicitly allow the visualization of the likelihood that a spacecraft has of being in a specific state. This state is represented by its position in the phase-space, i.e. altitude, velocity, and flight path angle but is not limited to it. In fact, the same information can be extracted for other useful quantities such as the impact range of the satellite that is its likelihood of landing in a certain location, or the heat load it must sustain during the different phases of the re-entry.

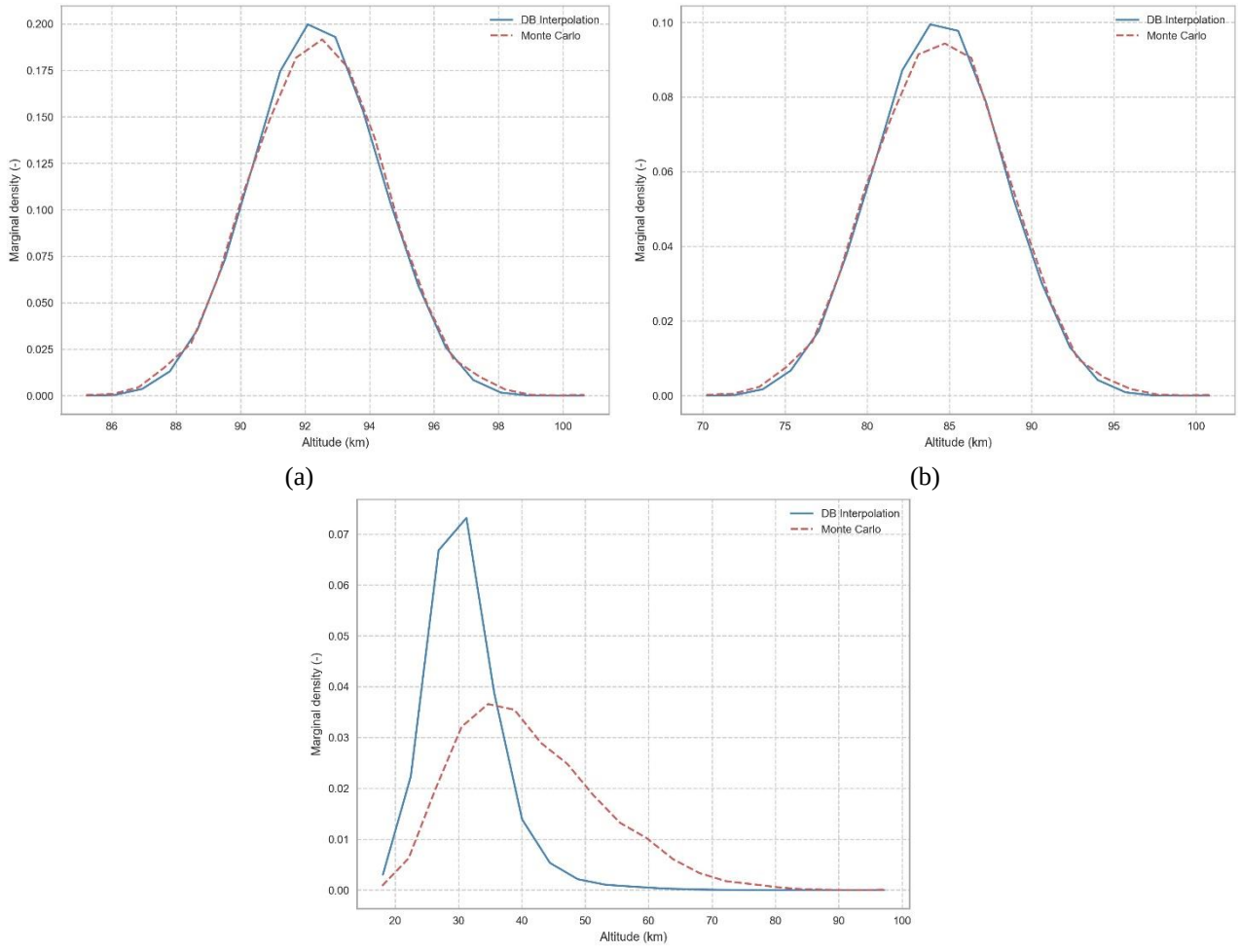

Figure 2. One-dimensional uncertainty marginal of the altitude at time t=40 s (a), t=80 s (b), and t=240 s (c). Comparison between the density-based triangulation (DB triangulation in the legend) and the MonteCarlo binning.

As these quantities are influenced by the state of the satellite, the uncertainty in the re-entry state and parameters propagates also on them. For example, knowing the uncertainty distribution of the heat load or the

mechanical load on the satellite can help extracting the probability distribution of the altitude at which the satellite breaks-up. Figure 2 and Figure 3 show examples of the one-dimensional and two-dimensional marginals that can be extracted by first performing the interpolation on the scattered data and then integrating Eq. (8) and Eq. (9), together with the equivalent distribution obtained using Monte Carlo binning. From the marginals in Figure 2, it is possible to observe that the distribution obtained through the density-based approach and the reconstruction through triangulation closely matches the one obtained with a Monte Carlo approach in the first two plots, corresponding respectively to a time instant of 40 s and 80 s. On the other hand, the plot (c) shows quite an evident difference between the two methods. Such a difference does not arise from the integration of the equations of motion and the density using the continuity equation and the method of characteristics, but in the post processing of the data through the interpolation method described in the Density reconstruction paragraph. A more detailed explanation of the reasons behind this difference is given in the Discussion section. Even the marginal in Figure 3 show a very similar behavior between the density-based and the Monte Carlo methodology, with the marginal having very good agreement up to 160 s of re-entry time. This indicates that the problematic in the reconstruction of the density through triangulation only begins in the latest stages of the re-entry, when the phase-space is highly deformed.

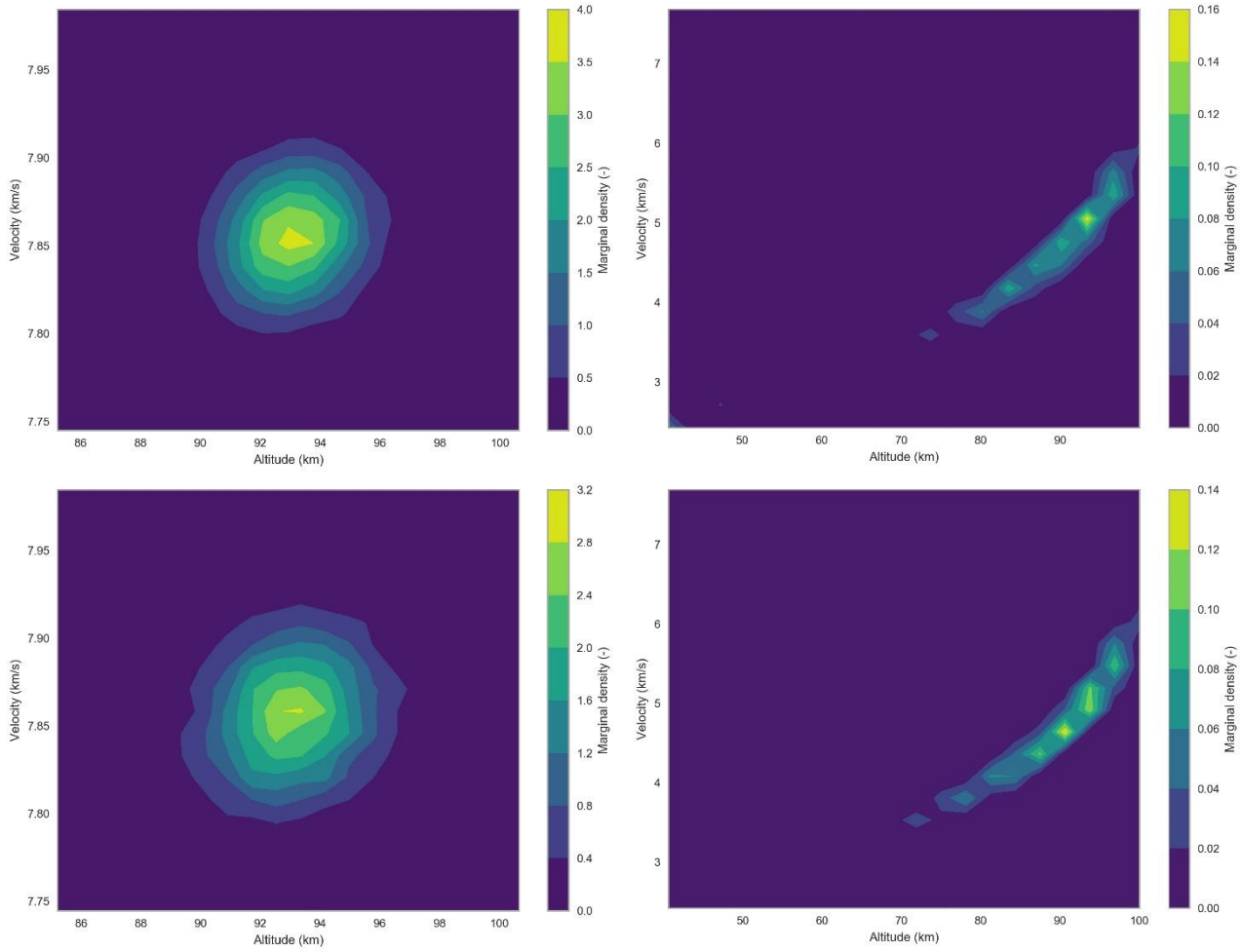

Figure 3. Two-dimensional uncertainty marginal of altitude and velocity. In the top row, the marginal obtained with the density-based method and the interpolation. In the bottom row, the equivalent marginal obtained with Monte Carlo binning. The first column refers to the time t=40 s and the second column to the time t=160 s.

As previously mentioned, an analogous procedure can be followed to obtain the marginals of other interesting quantities such as the heat load experienced by the spacecraft. Using the simplified relation of Eq. (10) the heat load has been estimated for each sample at each time step[10].

$$\dot{q} = \frac{1}{2} \cdot C_D \cdot \rho(h) \cdot V^3 \tag{10}$$

where ρ is the atmospheric density at the altitude h, C_D is the drag coefficient (assumed here equal to 2.2[10], and V is the velocity. Figure 4 shows an example of the obtained marginals after 40 s and 400 s, respectively.

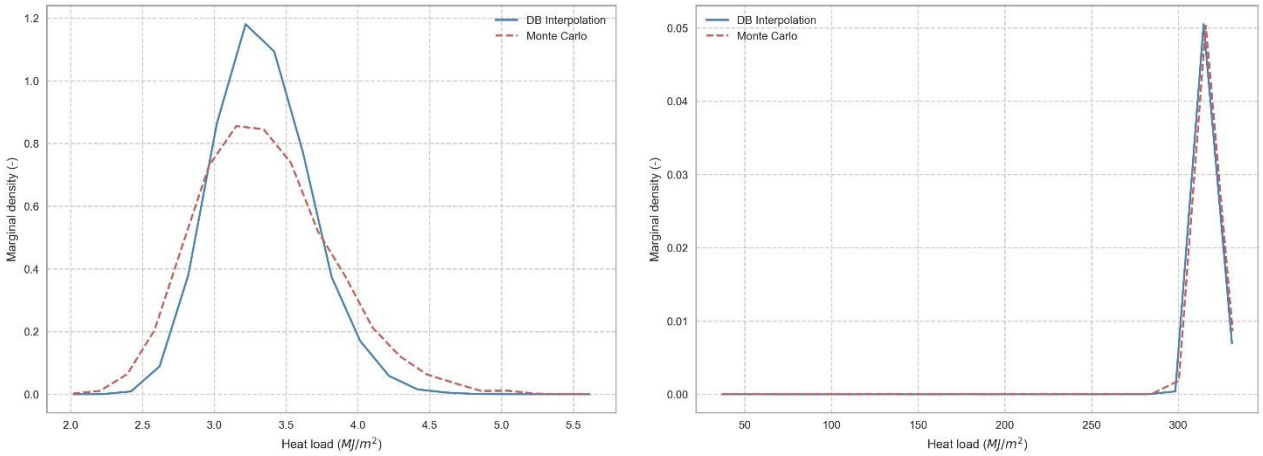

Figure 4. One-dimensional marginal of the heat load. On the left the heat load corresponding to the time t=40 s, and on the right the one corresponding to the time t=400 s.

Figure 5 shows a final marginal for the LEO return test case, which represents the probability distribution of the landing range of the spacecraft. The distribution represents the likelihood that the spacecraft would impact after the specified range. Both the density-based and the Monte Carlo methods predict that the peak probability corresponds to a landing range of 1600 km, with the density-based method having a higher peak and a lower variance for the impact location with respect to the Monte Carlo method. In general, the distributions predicted using the density-based method tend to have more localized peaks with reduced variance with respect to the correspondent Monte Carlo counterparts. This could be an expected behavior as in the density-based method we use the actual values of the uncertainties for each sample, thus having an exact evaluation of the uncertainties, even though it is only at specific points that are then used in the interpolation routine. On the other hand, the Monte Carlo based binning only provides an estimation of the probability density, which is usually under-predicted or over-predicted, especially when the number of samples is limited such as in this case.

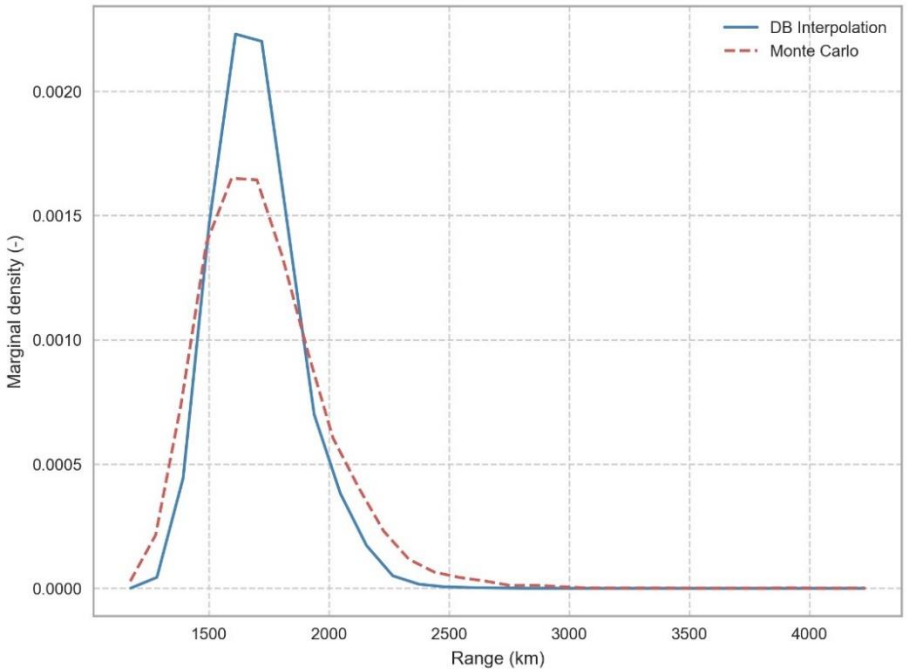

Figure 5. One-dimensional marginal for the landing range for the LEO re-entry.

The second test case presents a steep re-entry for a high ballistic coefficient satellite. In this case, as the satellite dives into the atmosphere with a large flight path angle (-30 degrees), the time of flight for the re-entry is significantly reduced and so is the time for the uncertainties to propagate as much as in the previous case. Figure 6 shows the evolution of the sampled points; in this case, the domain remains compact (left plot) only in the very first seconds of the re-entry, and quickly evolves into an elongate phase-space volume (right plot) after only 40 s into the re-entry process.

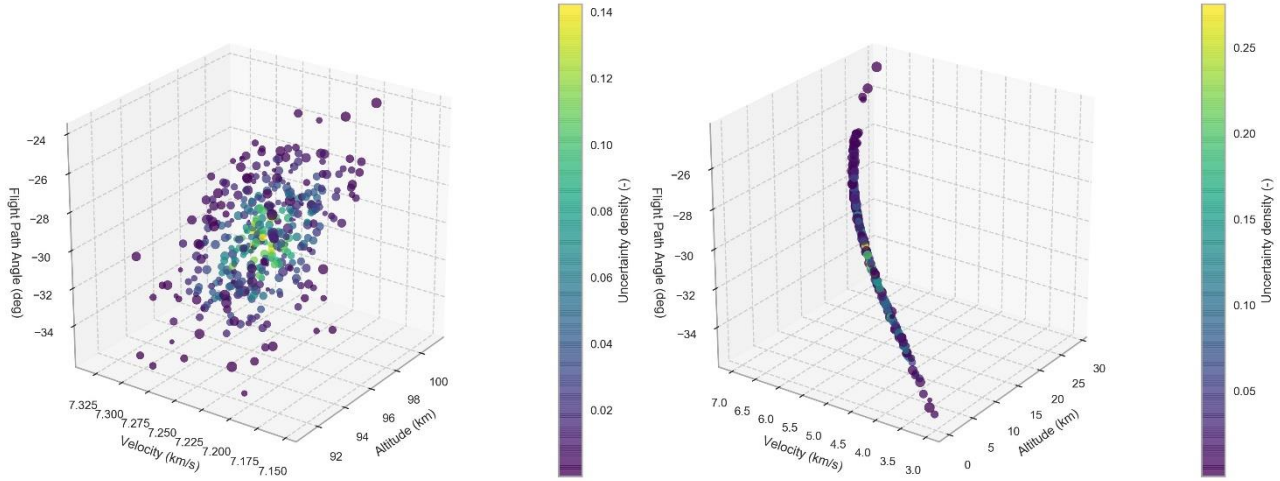

Figure 6. Scatter plot of the uncertainty evolution of the Strategic re-entry case for the sampled initial conditions and parameters. The left plot represent the re-entry after 8 s, the right after 40 s.

Similarly to the LEO case, we present also an example of one-dimensional altitude marginal (Figure 7) and the landing range marginal (Figure 8). In particular, Figure 8 shows how the uncertainties in the initial conditions and in the ballistic coefficient are less influential on the impact range for this case. In fact, as the re-entry has a significantly steeper trajectory, the propagation of the uncertainties is strongly reduced. Nonetheless, in this case, a strong agreement is maintained between the density-based and the Monte Carlo method throughout the entire simulation despite the deformation of the phase-space volume.

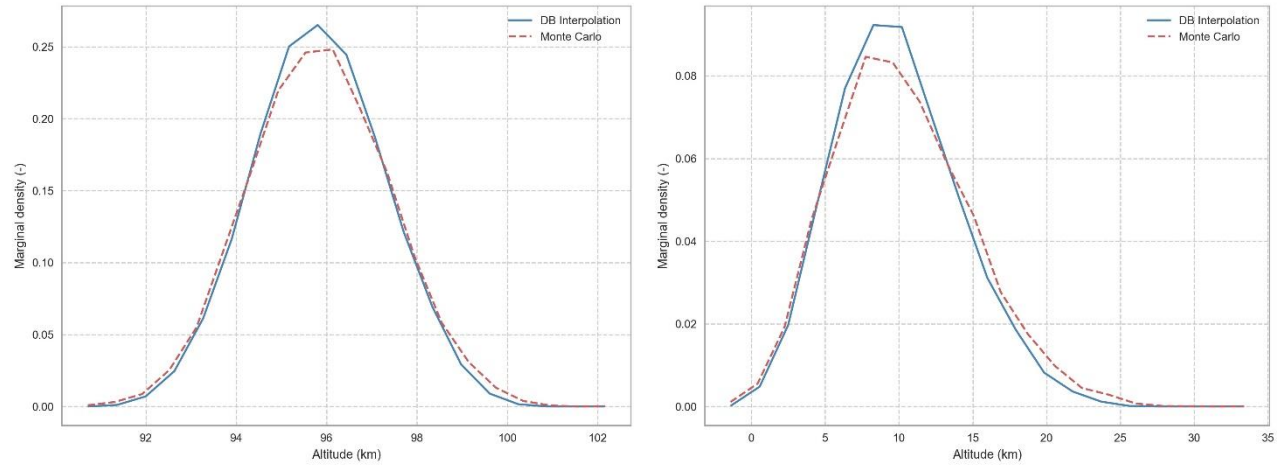

Figure 7. One-dimensional altitude marginals for the Strategic re-entry. The left plot represents the re-entry after 8 s, the right after 40 s.

This is an important aspect, as it highlights that it is not only important the shape of the phase-space volume but also its extension. In fact, in Figure 1 (bottom-right) the phase-space is considerably larger for all the variables thus introducing greater inaccuracy when applying the interpolation through the triangulation algorithm.

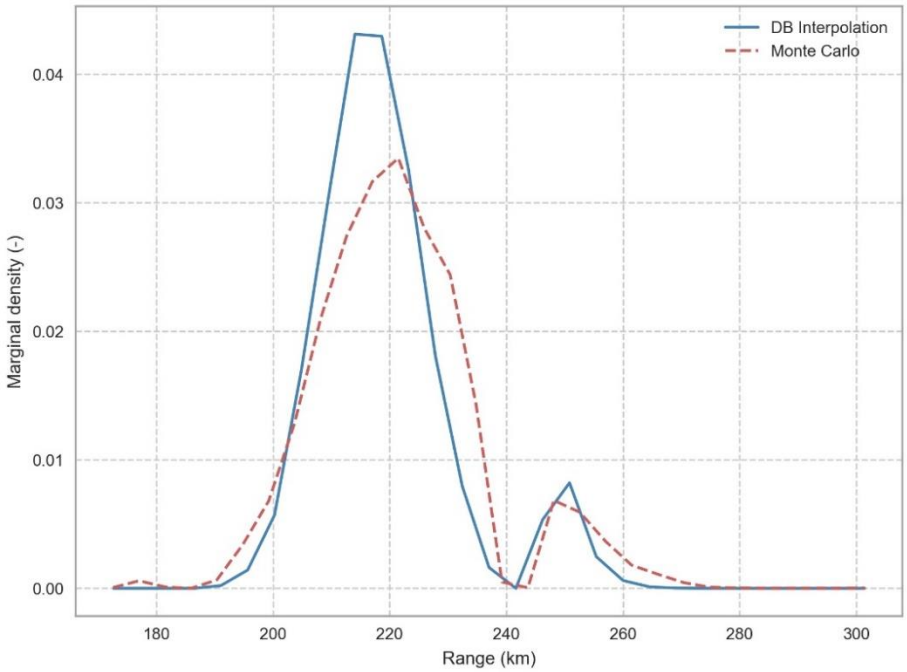

Figure 8. One-dimensional marginal for the landing range for the Strategic re-entry.

DISCUSSION

To highlight the differences between the two cases, and how these differences influence the reconstruction of the probability density and of the marginals, the result of the triangulation is presented for both cases at different time steps. In Figure 9, the blue dots represent the propagated samples and the red crosses represent the barycentres of the triangles created by the triangulation. The upper row refers to the LEO re-entry, while the lower row to the Strategic re-entry. The first column refers to an initial state of the re-entry with time instants t = 40 s and t = 8 s for the two re-entry cases respectively. The second column refers to a later stage of the re-entry with time instants t = 240 s and t = 40 s for the two cases respectively. From the plots on the left of Figure 9, it is clear how the generated triangulation closely follows the original samples, thus generating a proper interpolation of the data. On the other hand, the plots on the right show the creation of a set of points lying outside the region where the original samples are. They indicate that the triangulation is creating a set of unnecessary and unwanted triangles, which generate errors in the reconstruction of the probability density. This is due to the triangulation algorithm adopted: the Delaunay triangulation is, in fact, a reliable and efficient technique, which requires the creation of a convex hull in order to create the triangulation.

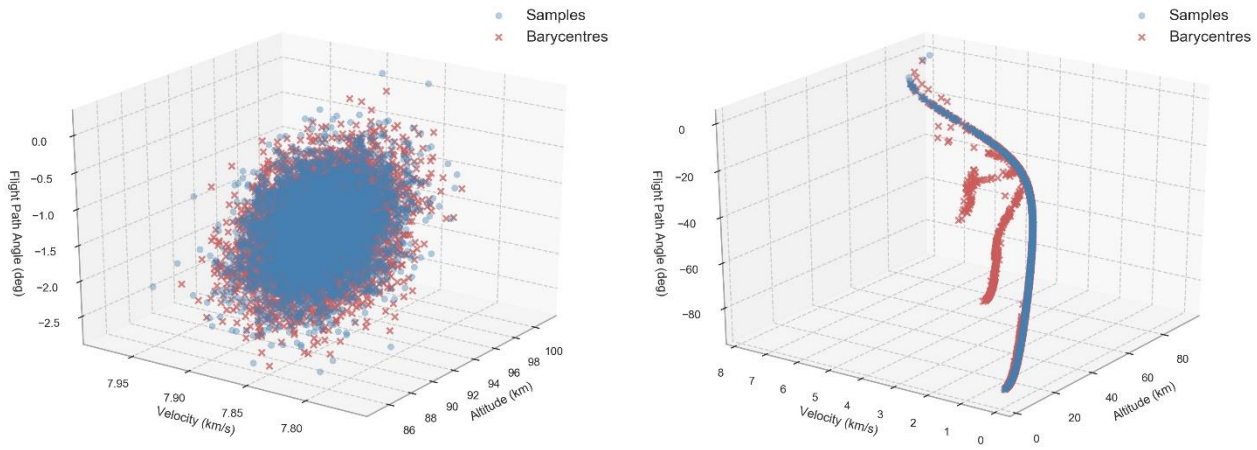

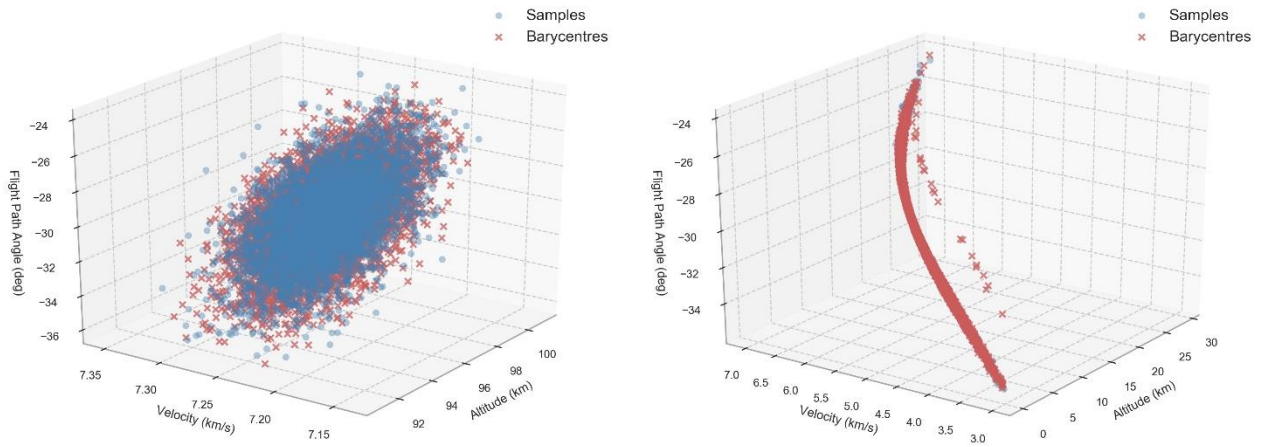

Figure 9. Scatter plot of the samples (blue dots) and of the barycentres generated by the triangulation (red crosses). The top rows refer to the LEO re-entry test case for the time instant t = 40 s (left) and t = 240 s (right). The bottom row refers to the Strategic test case for the time instant t = 8 s (left) and t = 40 s (right)

However, as the re-entry progresses, the phase-space deforms, and the domain does not maintain a characteristic of concaveness. Consequently, this introduces the interpolation errors previously mentioned and observable in Figure 2, plot (c).

The implementation of this methodology thus requires a procedure to prune all those triangles that have been added in order to fill the entire convex hull of the set of points. In other words, we need a methodology to compute the alpha-shape[11] of the set of points in order to perform the interpolation only using the meaningful simplexes and not the ones inadvertently introduced. As mentioned, such a methodology consists in finding the alpha shape of a set of points. For simplicity, let us consider a finite set of points S and a real positive number α. We define an open disk to be empty if it does not contain any point of S. Then, the α-hull is defined as the set of points that do not lie in any empty open disk of radius alpha. The definition of alpha-shape can then be extended to n-dimension considering instead of disks, n-dimensional spheres of radius α. At the current level of development, the implementation of the alpha-shape algorithm is limited to a three-dimensional space. Consequently, it has not been used in the previous computations. An example of the capability of implementing a pruning of the simplexes using alpha shapes is given in Figure 10. The plots represent the triangulation of the set of points corresponding to the LEO re-entry simulation at the time instant t = 80 s. On the left the standard Delaunay triangulation, while on the right the alpha-shape triangulation with an α value of 0.25. It is possible to observe that the use of the alpha-shape algorithm allows the removal of many of those unwanted simplexes.

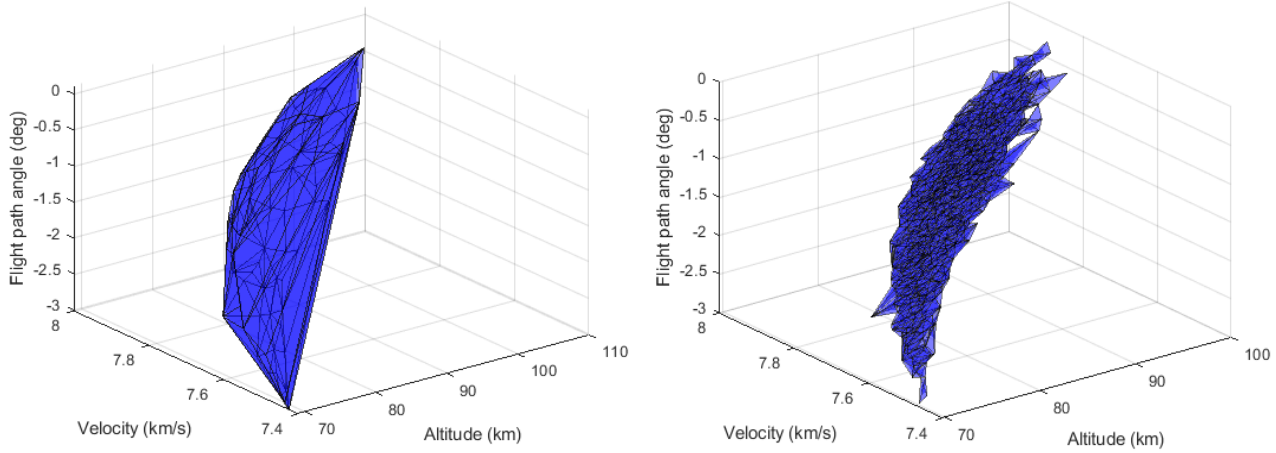

Figure 10. Application of the alpha-shape algorithm to the set of points of the LEO re-entry at time t = 80 s.

A drawback of such an implementation of the alpha-shape is the necessity to provide the parameter α, whose value is not easily guessed a priori and may require a trial-and-error procedure. Moreover, such a value of α, is univocal for the entire set of points, resulting in non-optimal pruning in certain locations, especially when the set of points is not uniformly distributed. In fact, it would be desirable, for example, to have an adaptive value of α as a function of the density of points and of the value of the probability density associated with the points. In such cases, the implementation of density-based alpha-shapes[12] could be adopted, improving both the results of the triangulation and removing the need for the user to select the value of α.

CONCLUSION AND FUTURE WORK

The presented work outlines a methodology to evaluate the effect of uncertainties in the re-entry of satellites without relying on computationally expensive Monte Carlo simulations, which become statistically meaningful only for high number of samples. The described methodology, instead, by directly propagating the probability density together with the equations of motion of the re-entry, allows the computation of the evolution of the actual uncertainty value for each of the sampled considered. Consequently, while the Monte Carlo approach estimates the uncertainties, the presented approach computes their actual values, thus allowing the reduction of the number of samples to be taken in order to have a statistically meaningful result. However, as we are interested in reconstruction the probability density and its marginal distributions on a thinner grid than the one used for the initial sampling, it is necessary to introduce a methodology that allows the computation of the density value in between the sampled points. This is achieved by linearly interpolating the set of scattered points obtained from the integration over the phase-space volume. With such a procedure, it is possible to extract the value of the density at any given point. For the purpose of this work, two test cases have been presented and the density-based method has been compared to the corresponding Monte Carlo method considering uncertainties in the initial conditions and in the ballistic coefficient of the satellites. This demonstrates the flexibility of the methodology, which allows the inclusion of both initial conditions and parameters of the re-entry as a source of uncertainty. The obtained results have been expressed in terms of one-dimensional and two-dimensional distribution of the relevant variables, comparing the developed methodology with the equivalent results of a Monte Carlo based binning. Alongside the probability distributions for the standard re-entry variables (altitude, velocity, and flight path angle), even the uncertainties related to other important quantities in the re-entry process, such as the heat load and the landing range have been presented. Of interest, the comparison between the two types of re-entry scenarios together with the exam of the marginals in the later stages of the simulations has revealed some issues with the direct implementation of a Delaunay triangulation for the interpolation. In fact, by using such triangulation scheme, unwanted simplexes are introduced in the triangulation of concave sets of points, thus leading to incorrect results. In conclusion, to the article, a solution has been proposed for the improvement of the linear interpolation using triangulation that is to introduce the concept of alpha-shapes. Such a concept, which is closely related to the one of convex hull, allows the pruning of the unwanted simplexes, thus improving the reliability and effectiveness of the interpolation. An example of the capability of alpha-shapes has been presented for a three-dimensional test case and the results have shown to be promising.

The presented methodology can be very powerful and, if carefully developed and tuned, can be extend to more dimensions (the presented case has four) including a complete six-state re-entry integration and the uncertainty of other parameters. Its possibility to significantly reduce the number of samples with respect to equivalent Monte Carlo techniques for uncertainty estimation has a great appeal, as well as the fact that what we obtain from the simulations are the actual values of the uncertainties and not an estimation. For the future development of the methodology, the first step is to build a reliable algorithm that can isolate the alpha-shape of the set of points even when the volume of the phase-space is highly deformed. Such an algorithm must also support n-dimensional spaces, as the other main objective of the methodology is to include as many dimensions as possible by considering the uncertainties in the initial conditions and in the parameters of the re-entry.

ACKNOWLEDGEMENT

This project has received funding from the European Research Council (ERC) under the European Union's Horizon 2020 research and innovation programme (grant agreement No 679086 - COMPASS).

REFERENCES

[1] A. Halder and R. Bhattacharya, "Dispersion analysis in hypersonic flight during planetary entry using Stochastic Liouville Equation," *Journal of Guidance, Control, adn Dynamics*, pp. 459-474, 2011.

[2] N. Gor'kavyi, “A new approach to dynamical evolution of interplanetary dust,” *Astrophysics Journal*, n. 474, pp. 496-502, 1997.

[3] C. R. McInnes, “An Analytical Model for the Catastrophic Production of Orbital Debris,” ESA Journal, Vol. 17, No. 4, 1993, pp. 293–305.

[4] L. Evans, “Partial Differential Equations,” American Mathematical Society, 1998.

[5] N. Gor'kavyi, “A new approach to dynamical evolution of interplanetary dust,” *Astrophysics Journal*, n. 474, pp. 496-502, 1997.

[6] Z. R. Putnam and R. D. Braun, “Extension and enhancement of the Allen-Eggers analytic solution for ballistic entry trajectories,” in *AIAA Atmospheric FLight Mechanics Conference*, Atlanta, 2014.

[7] D.-T. Lee, and B. J. Schachter. "Two algorithms for constructing a Delaunay triangulation," *International Journal of Computer & Information Sciences*, Vol. 9, Issue 3, pp. 219-242, 1980.

[8] P. Alfeld, "Scattered data interpolation in three or more variables," *Mathematical methods in computer aided geometric design*, pp. 1-33, 1989.

[9] M. Trisolini, H. G. Lewis, and C. Colombo. "Spacecraft design optimisation for demise and survivability," *Aerospace Science and Technology*, Vol. 77, pp. 638-657, 2018.

[10] C. Camilla, et al. "End-of-life Earth re-entry for highly elliptical orbits: the INTEGRAL mission," *The 24th AAS/AIAA space flight mechanics meeting*, 2014.

[11] E. Herbert. "Alpha shapes - a survey," *Tessellations in the Sciences* 27, pp. 1-25, 2010.

[12] T. Marek and M. Capps. "Surface reconstruction with anisotropic density-scaled alpha shapes," *Visualization'98. Proceedings*, IEEE, 1998.